A Reduced Order Steering State Observer for Automated Steering Control Functions

Enrico Raffone

FCA - Fiat Chrysler Automobiles, E/E & Connectivity Dept.,
Safety and Advanced Driver Assistance Systems – Control Systems, Strada Torino 50, 10043, Orbassano (TO), Italy

Keywords: Model based Estimation, Model Reduction, Kalman Filter, Singular Values, Least Square Model Identification, Observability Matrix, Singular Perturbation Balanced Model Reduction, Automotive, Steering System, Autonomous Vehicles.

Abstract: State observer design is one of the key technologies in research for autonomous vehicles, specifically the unmanned control of the steering wheel. Currently, estimation algorithms design is one of the most important challenges facing researchers in the field of intelligent transportation systems (ITS). In this paper we present: mathematical model and dynamic response identification of electric power steering column by least square identification experiments; observability analysis of identified models; model simplification via mechanical approach and singular perturbation model reduction; and two reduced order steering Kalman filter syntheses for estimation of steering column states and disturbances. The simulation and experimental results conducted on a steering test bench executed in the FCA Technical Center show that designed Kalman observers have good adaptability for steering wheel position control and safety aims. This can be useful in intelligent vehicle path tracking in outdoor experiments.

1 INTRODUCTION

Recent developments of automated vehicle technology have increased automation, efficiency, and safety in this field. The development of intelligent transportation systems (ITS) provides an opportunity to apply advanced technologies to systems and methods of transport for efficient, comfortable, and safer modes of transportation (i.e. highways, railways, inland waterways, airports, ports, etc.). The actual implementation of full automatic-steering control is one of most challenging disciplines in the intelligent-vehicles field. Perhaps this is the reason that it has a long way to go before it comes on the market. Currently, vehicle manufacturers focus on more mature systems, especially for speed control, some of which are already available on the market. There is, however, a short-term focus to steering control, not for unmanned lateral guidance, but as part of a driving assistance system, i.e. Lane Departure Warning system (also known as the Haptic Lane Feedback system) in use on Fiat Chrysler Automobiles. Automatic parking systems are other steering-control applications that are already on the market. All these systems exploit the preinstalled vehicle electric power-steering system to automatically manage the steering wheel for different purposes.

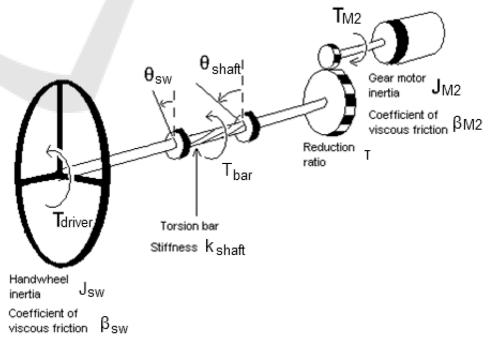

Figure 1: Electric Power Steering simplified mechanical model.

Automated steering control design is comprised of two main ways to design controllers: imitating human drivers or using dynamic models of cars and methods based on linear control theory. The first approach does not need detailed knowledge of car dynamics, much in the way the driver of a car does not. In this case, the algorithm key is the human

Raffone, E.
A Reduced Order Steering State Observer for Automated Steering Control Functions.
DOI: 10.5220/0005959704260432
In *Proceedings of the 13th International Conference on Informatics in Control, Automation and Robotics (ICINCO 2016) - Volume 1*, pages 426-432
ISBN: 978-989-758-198-4

driving behaviour. In the second approach, the control-system approach, it requires detailed knowledge of the dynamics of the car and in particular of the steering column. This paper focuses on the second approach, presenting solutions for steering control of autonomous vehicle developed by FCA Technical Center in steering control applications with an EPS steering actuator.

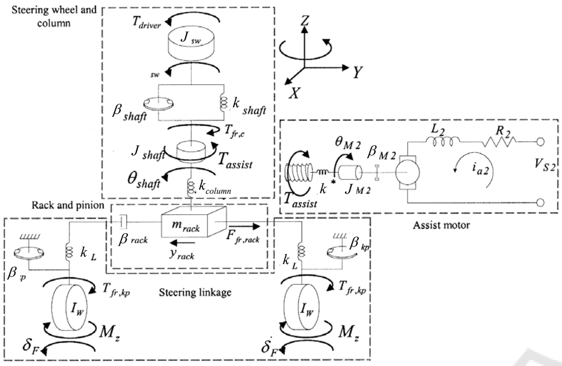

Figure 2: Free body diagram of electric assist rack and pinion steering system (Mills and Wagner, 2003).

2 ELECTRIC POWER STEERING COLUMN MODEL

2.1 EPS Mathematical Non-linear Model

The lumped parameter mathematical model for the high part of the steering column has been developed to investigate the dynamic behavior of steering column. In fig. 2 there is the free body diagram for steering column line and in particular EPS unit (Steering wheel, column, and assist motor diagrams). The differential equation for the steering wheel is:

$$J_{sw}\cdot\ddot{\vartheta}_{sw}+\beta_{shaft}\cdot\dot{\vartheta}_{sw}-k_{shaft}\cdot\left(\vartheta_{shaft}-\vartheta_{sw}\right)=T_{driver} \quad (1)$$

Now the shaft and gear-box rotational dynamics may be represented as:

$$\left(J_{shaft}+\tau^{2}\cdot J_{worm}\right)\cdot\ddot{\vartheta}_{shaft}=-k_{shaft}\cdot\left(\vartheta_{shaft}-\vartheta_{sw}\right)+k^{*}\cdot\left(\vartheta_{M2}-\tau\cdot\vartheta_{shaft}\right) \quad (2)$$

The dynamic equation for the motor angular displacement may be expressed as:

$$J_{M2}\cdot\ddot{\vartheta}_{M2}+\beta_{M2}\cdot\dot{\vartheta}_{M2}-k^{*}\cdot\left(\vartheta_{M2}-\tau\cdot\vartheta_{shaft}\right)=T_{M2}-T_{C} \quad (3)$$

where β_{M2} is the motor damping coefficient (see tab. 1 for other parameters).

Now, as said, the T_C term is the only Coulombian friction torque term in a mechanical configuration without any link to the low part of steering column, rack and pinion. With mechanical link, there is the disturbance torque from wheels (e.g. M_z) and, in addition, inertial and friction torques of low steering column.

The friction torque is modelled with a first order non-linear model known as Dahl friction model (Canudas-de-Wit et al., 2003). Dahl model was developed for simulating control systems with friction. The starting point of Dahl's model is the stress-strain curve in classical solid mechanics; see fig. 3. When subject to stress, the friction force increases gradually until rupture occurs. Dahl modelled the stress-strain curve by a differential equation.

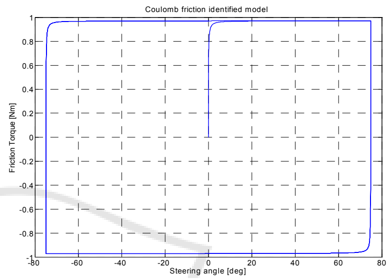

Figure 3: Identified Coulomb fiction nonlinear model.

Let ϑ be the relative angular displacement, $\dot{\vartheta}=d\vartheta/dt$ be the relative angular velocity, T the friction torque, and T_c the maximal friction force (Coulombian torque). Dahl's model takes the form (4),

$$\frac{dT}{d\vartheta}=\sigma\left(1-\frac{T}{T_c}\cdot \operatorname{sgn}\left(\dot{\vartheta}\right)\right)^{\alpha} \quad (4)$$

where σ is the stiffness coefficient (to be identified) and α is a parameter that determines the shape of the stress-strain curve. The value α = 1 is used in this work and also most commonly used.

All the model parameters are known from mechanical design of EPS unit except viscous damping parameters (β) and Coulomb friction nonlinear model parameters (σ e T_c) which are parameters identified by experimental data.

2.2 Least Square Model Identification

The identification activity used to define unknown parameters from a described model has been performed with an experimental test plan in particular proving conditions, e.g. with steering wheel locked or unlocked and without any mechanical link to rack and pinion steering system. This activity phase is accomplished by minimizing the least square error between model plant and measurement. So given a model family:

$$\mathrm{M} = \{M(\vartheta) \mid \vartheta \in \Theta\} \tag{5}$$

The parameters' vector ϑ, e.g. $\vartheta = [\beta_{vol}\ \beta_m\ \ \sigma]$, has been estimated using least square error minimization from real plant acquisitions $\{y_k, u_k\}_{k=1}^{N}$ in the admissible parameter set by minimizing the cost function:

$$J_N = \left(1/N\right) \cdot \sum_{k=1}^{N} \varepsilon_k^2 \tag{6}$$

Where ε_k is the error between simulation and plant acquisition at k_{th} sampling time.

In fig. 4 there is an example of matching between steering torque measured and simulated by identified model with the same motor torque input, a sweep with steering wheel locked. Then, a leave-one-out cross-validation of presented identified model has been performed in order to assess how the results of identification will generalize the real behaviour of steering unit.

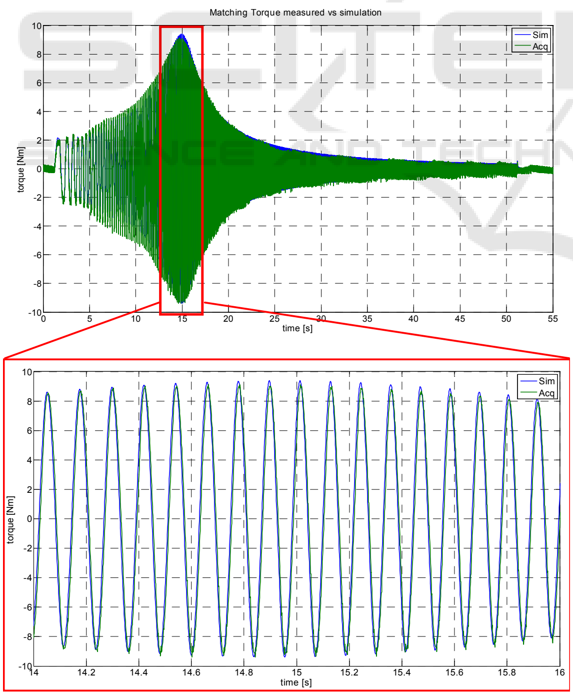

Figure 4: EPS model matching.

2.3 EPS Mathematical Linear Model

Already seen non-linear model may be linearized by eliminating Dahl frictional model. The frequency response of linear EPS model from motor torque to measured torque has been compared with frequency response obtained by an FFT analysis of time history data of the input and output (see fig. 5) in an interesting matching between data and linear model.

The classical space state representation for EPS linear model is:

$$\begin{cases} \dot{x} = A \cdot x + B \cdot u + B_d \cdot d \\ y = C \cdot x + D \cdot u \end{cases} \tag{7}$$

where:

$$x = [\dot{\vartheta}_{sw}\quad \dot{\vartheta}_{M2}\quad \dot{\vartheta}_{shaft}\quad \vartheta_{sw}\quad \vartheta_{M2}\quad \vartheta_{shaft}]^T;\ y = [\vartheta_{sw}\quad \vartheta_{M2}\quad T_{meas}]^T;$$
$$u = [T_{M2}];\ d = [T_{sw}\quad T_C]^T$$

and:

$$A = \begin{bmatrix} -\frac{\beta_{sw}}{J_{sw}} & 0 & 0 & -\frac{k_{shaft}}{J_{sw}} & 0 & \frac{k_{shaft}}{J_{sw}} \\ 0 & -\frac{\beta_{M2}}{J_{M2}} & 0 & 0 & -\frac{k^*}{J_{M2}} & \frac{k^* \cdot \tau}{J_{M2}} \\ 0 & 0 & 0 & \frac{k_{shaft}}{J_{shaft} + J_{worm} \cdot \tau^2} & \frac{k_{shaft} \cdot \tau}{J_{shaft} + J_{worm} \cdot \tau^2} & \frac{-k_{shaft} - k^* \cdot \tau^2}{J_{shaft} + J_{worm} \cdot \tau^2} \\ 1 & 0 & 0 & 0 & 0 & 0 \\ 0 & 1 & 0 & 0 & 0 & 0 \\ 0 & 0 & 1 & 0 & 0 & 0 \end{bmatrix}$$

$$B = \begin{bmatrix} 0 \\ 1/J_{M2} \\ 0 \\ 0 \\ 0 \\ 0 \end{bmatrix};\ B_d = \begin{bmatrix} 1/J_{sw} & 0 \\ 0 & -1/J_{M2} \\ 0 & 0 \\ 0 & 0 \\ 0 & 0 \\ 0 & 0 \end{bmatrix};\ C = \begin{bmatrix} 0 & 0 & 0 & -k_{shaft} & 0 & k_{shaft} \\ 0 & 0 & 0 & 1 & 0 & 0 \\ 0 & 0 & 0 & 0 & 1 & 0 \end{bmatrix};\ D = 0.$$

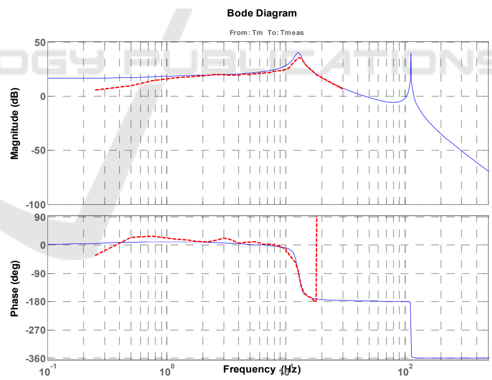

Figure 5: EPS bode diagram from linear model (continuous line), from FFT data analysis (dotted line).

Table 1: Units for EPS mathematical model.

Symbol	Description	Unit
J_{sw}	Steering wheel moment of inertia	[Kgm^2]
β_{sw}	Steering wheel viscous damping	[Nms/rad]
k_{shaft}	Torsion bar spring rate	[Nm/rad]
k_{column}	Steering column stiffness	[Nm/rad]
k^*	Motor-gear coupling stiffness	[Nm/rad]
β_{M2}	Motor viscous damping	[Nms/rad]
J_m	Motor rotor moment of inertia	[Kgm^2]
J_{shaft}	Gear-box wheel moment of inertia	[Kgm^2]
J_{worm}	Gear-box worm moment of inertia	[Kgm^2]
T	Gear-box ratio	-

3 EPS MODEL OBSERVABILITY

3.1 Observability Vs Plant Measures

Observability, in control theory, is a measure of how well internal states of a system can be inferred by knowledge of its external outputs. Less formally, this means that from the system outputs it is possible to determine the behavior of the entire system. If a system is not observable, this means the current values of some of its states cannot be determined through output sensors. So, an interesting thing about EPS mechatronic architecture is to understand the level of observability in front of minimum number of plant measures.

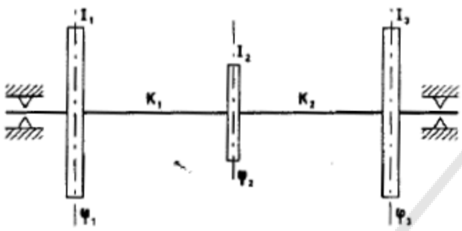

Figure 6: EPS mechanical outline.

The EPS column mechanical outline can be modelled as in fig. 6, where according to C measures matrix in (7) the available measures are: steering flywheel position (φ_1), EPS motor flywheel position (φ_3) and torque measure T_{bar} as difference between gear box output shaft (φ_2) and steering wheel position (φ_1) multiplied for known torsion bar stiffness (K_1).

From the classical analysis of observability matrix rank (see tab. 2), it's clear that only two of three measures are fundamental for full observability of system modes. The presence of three different measurements is principally due to safety reasons. A single measure for steering or motor flywheel position is enough to observe five of six states. Measured torque T_{bar}, seen as a relative position difference gives a reduced level of observability, only four states.

Table 2: EPS system observability vs plant measures.

T_{bar}	θ_{sw}	θ_{M2}	Observability Order
-	-	-	0
-	-	√	5
-	√	-	5
-	√	√	6
√	-	-	4
√	-	√	6
√	√	-	6
√	√	√	6

3.2 Spectral Decomposition for Linear Model

The spectral decomposition of state matrix A is a simple method to know all dynamics in the real plant. In tab. 3, the eigenvalues for our linear model, it's clear that the model plant is characterized by the presence of very low and high frequency terms.

Table 3: EPS linear model eigenvalues.

Eigenvalues	*Freq. [Hz]*
-0.491074732452 + 706.750702094704i	112.5
-0.491074732452 - 706.750702094704i	112.5
-0.000000000001	0.000…
-8.114907494361	1.3
-3.839922431729 + 79.657898579634i	12.7
-3.839922431729 - 79.657898579634i	12.7

3.3 Observability with Disturbances Addition

To observe disturbance inputs from driver torque and disturbance torque from wheels, the described model plant has been extended with two additional states, T_{driver} and T_c, considered as Gaussian processes with zero means.

The observability was evaluated with these two additional states. The new state matrix A has dimensions 8x8, and now includes also the terms in B_d matrix (7). New states vector is:

$$x = \left[\dot{\vartheta}_{sw} \quad \dot{\vartheta}_{M2} \quad \dot{\vartheta}_{shaft} \quad \vartheta_{sw} \quad \vartheta_{M2} \quad \vartheta_{shaft} \quad T_{driver} \quad T_C\right]^T \qquad (8)$$

But now, rank of observability matrix is only 5, this because new state space model is ill-conditioned. It's due to numerical problems linked to the presence of very different numeric parameter entities, i.e. small gear-box inertial term in front of steering wheel one, or torsion bar stiffness in front of motor-gear joint coupling stiffness, etc. The only possibility to estimate system states and disturbances is to simplify the model structure, eliminating unnecessary high frequency dynamics, in practice gearbox dynamics which are over 100 Hz, out of frequency range of interest.

4 EPS MODEL ORDER REDUCTION

Approaches for model reduction reflect two different points of view: a mechanical approach and a singular values approach. The first action is to eliminate defined dynamics considering equivalent inertial effects and stiffness. In the second approach, the action is to improve observability and controllability of the model by using an orthogonal base change in order to reach a new linear combination of system states (a balanced realization) and then to eliminate the new states with weak singular values, so less observable (singular perturbation reduction method (Moore, 1981); (Fernando et al., 1982); (Liu at al., 1989); (Saksena et al., 1984)).

4.1 Mechanical Approach

The basic idea is to simplify the model plant, starting from this equality:

$$\vartheta_{shaft} = \frac{\vartheta_{M2}}{\tau} \quad (9)$$

Then, defining an equivalent inertia for EPS motor:

$$J_{M2_{new}} = J_{M2} + J_{worm} + \frac{J_{shaft}}{\tau^2} \quad (10)$$

And an equivalent stiffness for torsion bar:

$$k_{shaft_{new}} = k_{shaft} + \frac{k^*}{\tau} \quad (11)$$

The new differential equation for steering wheel is:

$$J_{sw} \cdot \ddot{\vartheta}_{sw} + \beta_{shaft} \cdot \dot{\vartheta}_{sw} - k_{shaft_{new}} \cdot \left(\frac{\vartheta_{M2}}{\tau} - \vartheta_{sw} \right) = T_{driver} \quad (12)$$

And new rotational dynamics for EPS motor:

$$J_{M2_{new}} \cdot \ddot{\vartheta}_{M2} + \beta_{M2} \cdot \dot{\vartheta}_{M2} + \frac{k_{shaft_{new}}}{\tau} \cdot \left(\frac{\vartheta_{M2}}{\tau} - \vartheta_{sw} \right) = T_{M2} - T_C \quad (13)$$

So, the reduced order model is based only on (12) and (13), in practice the same identified model with no gear box dynamics represented.

4.2 Singular Perturbation Balanced Model Reduction

The balanced representation technique developed in (Saksena et al., 1984) is used as a basic tool for deriving acceptable reduced-order model for the dynamic analysis/synthesis on EPS system. In a balanced representation, the controllability and observability gramians, which represent the input-state and output-state maps, respectively, are equal and diagonal. The diagonal entries of these gramians, called the singular values, measure the degree of controllability and observability of the states in this representation. The balanced representation may be partitioned into the following two interconnected systems:

1. *the dominant subsystem:* most controllable and most observable part corresponding to large singular values;
2. *the non-dominant subsystem:* the least controllable and least observable part corresponding to small singular values.

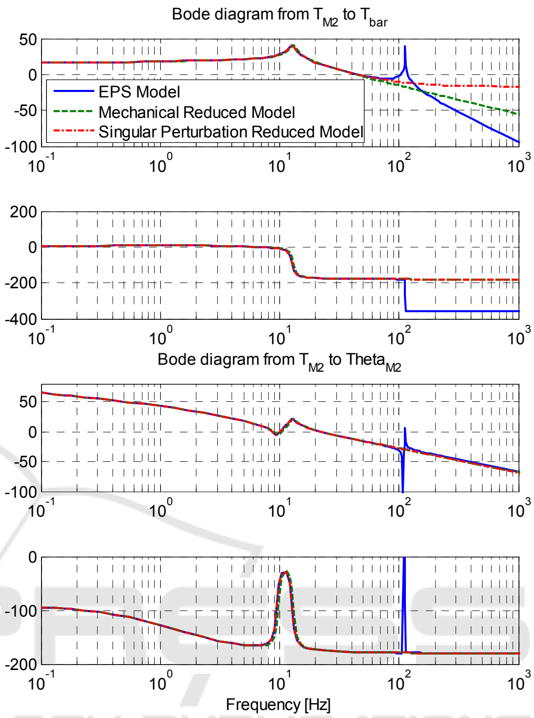

Figure 7: EPS reduced models compare.

The most controllable and most observable states, corresponding to the singular values of the largest magnitudes, are retained in the reduced model.

Then singular perturbation method is an effective method at low frequency for reducing large scale systems. Singular perturbation approximation of balanced systems was addressed by several investigators (Fernando et al., 1982); (Liu at al., 1989); (Saksena et al., 1984). The basic algorithm can be summarized as follows:

1. Transform the system in Eq. (7) into the balanced representation:

$$\begin{bmatrix} \dot{\tilde{x}}_1 \\ \dot{\tilde{x}}_2 \end{bmatrix} = \begin{bmatrix} A_{11} & A_{12} \\ A_{21} & A_{22} \end{bmatrix} \cdot \begin{bmatrix} \tilde{x}_1 \\ \tilde{x}_2 \end{bmatrix} + \begin{bmatrix} B_1 \\ B_2 \end{bmatrix} \cdot u$$
$$y = \begin{bmatrix} C_1 & C_2 \end{bmatrix} \cdot \begin{bmatrix} \tilde{x}_1 \\ \tilde{x}_2 \end{bmatrix} \quad (14)$$

Where: $\tilde{x} = T \cdot x$ is new balanced states vector, $\tilde{x}_1$ is system states vector strongly controllable and observable and $\tilde{x}_2$ is system states vector weakly controllable and observable.

2. Now (A_{11}, B_1, C_1) represent the strong subsystem and (A_{22}, B_2, C_2) represent the weak subsystem.
3. Calculate the reduced-order model

$$\begin{cases} \dot{x}_1 = \overline{A}_{11} \cdot x_1 + \overline{B}_1 \cdot u \\ y = \overline{C}_1 \cdot x_1 + \overline{D}_1 \cdot u \end{cases} \tag{15}$$

as follows:

$$\begin{aligned} \overline{A}_{11} &= A_{11} - A_{12} \cdot A_{22}^{-1} \cdot A_{21} \\ \overline{B}_1 &= -A_{12} \cdot A_{22}^{-1} \cdot B_2 + B_1 \\ \overline{C}_1 &= C_1 - C_2 \cdot A_{22}^{-1} \cdot A_{21} \\ \overline{D}_1 &= -C_2 \cdot A_{22}^{-1} \cdot B_2 \end{aligned} \tag{16}$$

In this new reduced order model obtained above, the steady-state error has been completely eliminated.

5 REDUCED ORDER EPS STATES KALMAN OBSERVER

Now with either of the reduced order models, the rank of observability matrix contains also additional disturbances. These models have been used to synthesize two different linear stationary Kalman observers with estimation of EPS states in a potential state-feedback control framework. Using a common space-state model (17) derived from (12) and (13) equations for mechanical approach and (15) for singular perturbation reduced balanced model:

$$\begin{cases} \dot{x} = \tilde{A} \cdot x + \tilde{B} \cdot u + \gamma \cdot \xi \\ y = \tilde{C} \cdot x + \upsilon \end{cases} \tag{17}$$

Where ξ and υ are respectively assumed Gaussian process and measurement white noises with zero means. Now the state variables are:

$$x = \begin{bmatrix} \dot{\vartheta}_{sw} & \dot{\vartheta}_{M2} & \vartheta_{sw} & \vartheta_{M2} & T_{driver} & T_C \end{bmatrix}^T \tag{18}$$

and measures:

$$y = \begin{bmatrix} \vartheta_{sw} & \vartheta_{M2} & T_{bar} \end{bmatrix}^T \tag{19}$$

Remember that system states vector for mechanical approach is the same of full model excluding weak states, so exactly the states vector (18), while the states vector for singular perturbation method is a linear combination of original physical states. It's fundamental to take into account the states transformation from original realization to this balanced and reduced realization in order to reconstruct original physical states.

About observers gains synthesis (L matrix in fig. 8), all the process state variables are considered Gaussian stochastic ones, so the assumed noise covariance matrix has been defined in coherence with physical characteristics of relative stochastic variables and then tuned in order to get the best estimation possible.

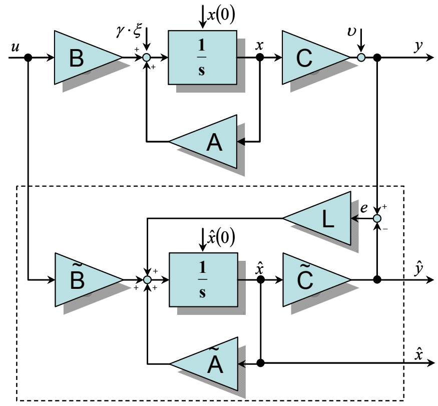

Figure 8: Linear Kalman Observer block diagram.

Figure 9: FCA Innovation Technical Center EPS test bench.

6 OBSERVERS TEST ON EPS TEST BENCH

A comparative test was performed on the FCA Technical Center EPS test bench (see fig. 9) with a first attempt linear quadratic regulator (LQR) to realize a closed loop control of EPS output shaft position. Developed state-feedback control uses estimated/filtered system states: angular speeds and positions; while steering wheel estimated torque disturbance is used for safety reasons to understand if a potential driver puts his hands on the steering wheel during unmanned lateral control of a vehicle.

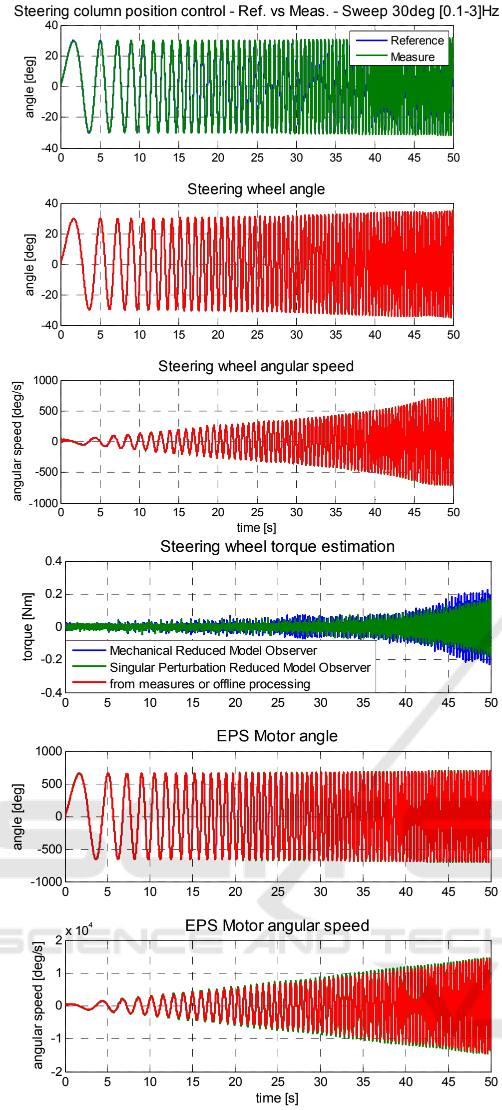

Figure 10: Estimation test on EPS test bench.

In the graphs (see fig. 10), a comparison between controlled steering column angular position reference and measure (1st graph), then steering wheel position (measured vs filtered) (2nd graph) and steering angular speed (estimated vs offline calculated one) (3rd graph), steering wheel torque estimation signals (4th graph) from two synthesized observers, steering wheel and EPS motor filtered/measured angles (5th graph) and estimated angular speeds and offline processed ones from angular measurements (6th graph), so with no delay, during a sweep of EPS output shaft position (amplitude 30deg, frequency range [0.1, 3]Hz). Fig. 10 shows very interesting estimation results in front of real measured signals and offline processed ones.

This test, as other tests carried out on the EPS bench, have demonstrated the effectiveness of these two observers as two interchangeable intelligent algorithms developed for exploiting different physical and numerical methods to observe optimal EPS states.

7 CONCLUSIONS

Simple linear models/observers/controllers are normally preferred over complex ones in control system design for an obvious reason; they are much easier to do analysis and synthesis with. This paper demonstrates the utility and effectiveness of intelligent algorithms for the steering state estimation based on reduced order models. The mechanical approach is an effective method to reduce model plant when this model is well known. The singular perturbation balanced model reduction is a formidable tool which is more numerical and useful to improve controllability or observability of plant and finally to reduce model plant according to a ‘singular values rule’. The main paper results are two interchangeable Kalman observers useful for the estimation of steering line states in order to control steering wheel position. Next developments are as follows: identification of disturbance from low part of steering line in different conditions, and control of electric power steering unit with optimal linear state-feedback control approach.

REFERENCES

V. D. Mills, J. R. Wagner, 2003. “Behavioural modelling and analysis of hybrid vehicle steering systems”, in *Proceedings of the Institution of Mechanical Engineers Part D-Journal of Automobile Engineering*.

C. Canudas-de-Wit, P. Tsiotras, E. Velenis, M. Basset, G. Gissinger, 2003. “Dynamic Friction Models for Road/Tire Longitudinal Interaction” in *Vehicle System Dynamics*, Volume 39, Issue 3.

Moore B.C., 1981. “Principal component analysis in linear systems: controllability, observability, and model reduction”, in *IEEE Trans Autom Contr*, AC-26.

Fernando K.V., Nicholson H., 1982. “Singular perturbation model reduction of balanced systems”. In *IEEE Trans Autom Contr*, AC-27.

Liu Y., Anderson BDO, 1989. “Singular perturbation approximation of balanced systems”. In *Int J Contr*.

Saksena V.R., O'Reilly J., Kokotovic P.V., 1984. “Singular perturbations and time scale methods in control theory: survey 1976±1983. In *Automatica*.

Kalman, R. E., 1960. “A New Approach to Linear Filtering and Prediction Problems”. In *Transactions of the ASME, Journal of Basic Engineering*, Pg. 35-45.